Distorted field scattering in a nanoscale MOSFET in the ballistic transport regime

2007 J. Phys.: Condens. Matter 19 446208

(http://iopscience.iop.org/0953-8984/19/44/446208)

IOP PUBLISHING JOURNAL OF PHYSICS: CONDENSED MATTER

J. Phys.: Condens. Matter **19** (2007) 446208 (10pp) doi:10.1088/0953-8984/19/44/446208

Distorted field scattering in a nanoscale MOSFET in the ballistic transport regime

K-M Hung[1], J-H Dai[1], K-Y Wu[1], W Y Tso[1], J-T Chen[1], K-Y Horng[2] and T-H Shieh[3]

[1] Department of Electronics Engineering, National Kaohsiung University of Applied Sciences, 415, Chien-Kung Road, Kaohsiung, 807, Taiwan, Republic of China
[2] Solid State Device Section of the Electronic System Research Division, Chung-Shan Institute of Science and Technology, PO Box 90008-22-11, Lungtan, Taoyuan, 32599, Taiwan, Republic of China
[3] Department of Electronics Engineering, Kun Shan University, 949, Dawan Road, Yung-Kang City, Tainan Hsien, 710, Taiwan, Republic of China

E-mail: kmhung@cc.kuas.edu.tw

Received 17 April 2007, in final form 30 September 2007
Published 16 October 2007
Online at stacks.iop.org/JPhysCM/19/446208

Abstract

This investigation studies theoretically transmissions and conducting currents in a nanometre field effect transistor in a distorted electric field. In the ballistic transport regime, the momentum conservation does not apply in the direction perpendicular to the carrier transport owing to the presence of a distorted electric field that is caused by the drain and gate biases associated with the fringe effect. This scattering occurs in both long- and short-channel field effect transistors, and is particularly large in nanometre devices that operate in the ballistic transport regime.

(Some figures in this article are in colour only in the electronic version)

1. Introduction

Recently, technology for the mass production of semiconductor devices has reached the milestone of manufacturing a metal–oxide–semiconductor field effect transistor (MOSFET) with a gate length of 45 nm. Further advances will shrink the gate length to 30 nm or even smaller [1, 2]. Ballistic transport and quantum transport [1, 3–5] are important when the gate length is comparable to or smaller than the mean free path (which depends on the doping concentration in the conducting channel, the operating temperature, the defect density, the oxide charge [6] and the doping concentration in the poly-gate for a very thin oxide [7], $<$1.7 nm) and the Fermi wavelength of the conducting carriers in the channel material. However, the combination of the drain (V_D) and gate (V_G) biases associated with

the fringe effect[4] produces a distorted field (DF)—a field strength in the direction normal to the conducting channel that is a function of the distance along the channel. The distorted field acts as a scattering source to the conducting carriers, and becomes gradually more important as the device is shrunk, especially in the scattering-free or ballistic transport regime. This work reveals that the scattering strength of DF, according to the multi-channel transfer matrix (MT) method [8–10], is significant in the nanoscale MOSFET (ns-MOS), and should change the transmission and conducting current in the high DF regime.

In theoretical investigations, the Green's function (GF) approach has been widely used in the study of the transport characteristics of ns-MOS devices [11–14]. The advantages of the GF approach are: (1) detailed information on system wavefunctions is unnecessary; and (2) it has been well developed to treat interacting systems [15, 16], such as carrier–carrier, carrier–phonon and carrier–impurity interactions. In highly non-equilibrium regime, where the Fermi–Dirac distribution is no longer applicable, instead, the non-equilibrium GFs have to be considered and make numerical calculation complicated. The transfer matrix method, based on the basis of system wavefunctions, is one of the useful methods in the investigation of quantum transport. The convenience of the method is that the detailed distribution in the non-equilibrium regime is inessential, because the carrier concentration in that regime can be directly deduced from the source reservoirs, which are in equilibrium, through the connection of the system wavefunctions. In this work, the transfer matrix theory was extended to the case of multiple conducting channels with the presence of a scattering potential (DF scattering). A comparison between the transmissions estimated using MT and GF approaches for an ns-MOS without the presence of DF is also presented.

Section 2 of this work first discusses multi-channel quantum transport theory for an ns-MOS. Section 3 presents numerical results and discusses an ns-MOS with a gate length of 10 nm. Finally, section 4 draws conclusions.

2. Theory

To demonstrate the DF scattering, consider an ns-MOS structure that is built on an SOI (silicon on insulator) wafer, as displayed in figure 1, and composed of a heavily doped source and drain, an undoped channel with a channel length of L and a channel height of H, and a gate that is capacitively coupled to the conducting channel. Although this single-gate structure will not be the device architecture of choice for ultimate scaling, it is convenient for demonstrating the DF scattering in an ns-MOS without loss of generality. The heavy doping of the source and drain allow them to be treated as reservoirs. In the one-band effective-mass approximation, the system can be described using a three-dimensional Schrödinger equation,

$$-\frac{\hbar^2}{2}\vec{\nabla}\cdot\left(\frac{1}{m^*}\vec{\nabla}\Psi\right)+V(x,y,z)\Psi=E\Psi, \tag{1}$$

where the potential V includes the external biases and the potential of the structure that confines the carriers in the z-direction with an infinite barrier height but allows them to be transported in the y-direction and to move freely in the x-direction, and m^* is the effective mass of the carriers. The undoped Si channel associated with the heavily doped source and drain forms a square barrier V_{y0} between the source and the drain with barrier height $E_g/2 + E_f$, where E_g is the forbidden gap of Si and E_f is the Fermi energy in the source and drain regions. In the

[4] The fringe effect in ns-MOS results in a non-uniform electric field in the channel, which not only corrects the capacitance of the parallel-plate capacitor between the gate and source/drain, but also reduces the field effect of the gate bias and provides a distorted field as well.

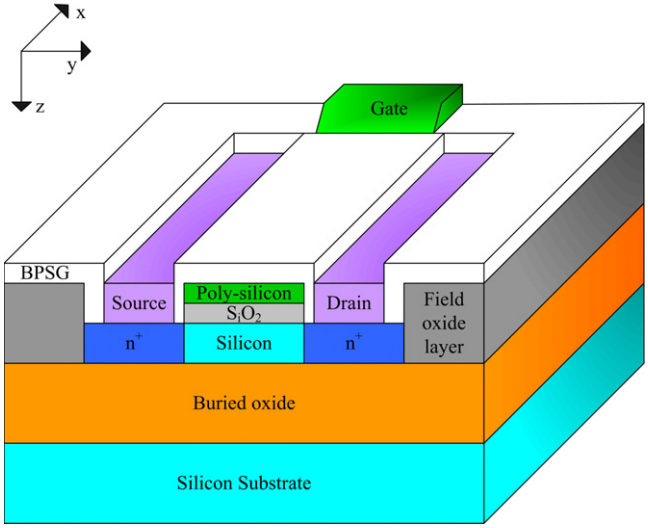

Figure 1. Schematic structure of the ns-MOS.

gradual channel approximation [6], the model potential V has the simple form

$$V = \begin{cases} V_{z0} & \text{for } y \leqslant 0 \\ -\dfrac{eV_D}{L}y - \dfrac{e\varepsilon_{ox}}{(\varepsilon_{Si}d + \varepsilon_{ox}H)}\left(\dfrac{V_{Geff}}{L/2} - \dfrac{V_D}{L}\right)(H-z)y & \\ \quad + V_{y0} + V_{z0} & \text{for } 0 < y \leqslant L/2 \\ -\dfrac{eV_D}{L}y - \dfrac{e\varepsilon_{ox}}{(\varepsilon_{Si}d + \varepsilon_{ox}H)}\left(\dfrac{V_{Geff}}{L/2} - \dfrac{V_D}{L}\right)(H-z)(L-y) & \\ \quad + V_{y0} + V_{z0} & \text{for } L/2 < y \leqslant L \\ -\dfrac{eV_D}{L}y + V_{z0} & \text{for } L < y, \end{cases} \tag{2}$$

where ε_{ox} (ε_{Si}) is the dielectric constant of SiO_2 (Si), V_{z0} is the square-well potential with an infinite barrier height in the z-direction, and V_{Geff} is the effective gate bias that includes the effects of the oxide charge and work-function difference between the metal gate and the Si channel. The drain bias V_D drives the charge particles through the conducting channel. In the channel region $0 < y \leqslant L$, the potential V includes the effect of DF that depends on the channel length, the channel height, the gate oxide thickness d, the biases V_D and V_{Geff}, the distribution of space charge and the geometry of the device. In the model potential that is described by equation (2), the screening-free DF potential[5] has the form

$$V_{DF} = e\varepsilon(y)z = \begin{cases} 0 & \text{for } y \leqslant 0 \\ \dfrac{e\varepsilon_{ox}}{(\varepsilon_{Si}d + \varepsilon_{ox}H)}\left(\dfrac{V_{Geff}}{L/2} - \dfrac{V_D}{L}\right)yz & \text{for } 0 < y \leqslant L/2 \\ -\dfrac{e\varepsilon_{ox}}{(\varepsilon_{Si}d + \varepsilon_{ox}H)}\left(\dfrac{V_{Geff}}{L/2} - \dfrac{V_D}{L}\right)yz & \text{for } L/2 < y \leqslant L \\ 0 & \text{for } L < y. \end{cases} \tag{3}$$

[5] The screening effect redistributes the charge distribution in the conducting channel and thus enhances the local electric fields in both y- and z-directions. This may result in strengthening local DF strength, especially in nanoscale devices where the ballistic transport dominates the device's characteristics. Therefore, a screening-free potential is good for demonstrating the effect of DF scattering.

In the absence of the DF potential, the transverse momentum of the transporting carriers is conserved as they pass through the structure—no scattering occurs; but a non-zero distorted field alters the direction of the momentum of the carriers from their transverse states to another state but conserves the absolute momentum; elastic scattering occurs.

Equation (1) is solved by applying the one-dimensional finite-element approach to the y-directional potential, where the structure along the y-axis is partitioned into $N+1$ layers, each with a y-independent potential $V_i((y_i + y_{i+1})/2, z)$, where y_i is the location of the ith interface between the ith and $(i-1)$th layers. During this treatment, the potential V of the ith layer has the form $V_i = V_{0i} + e\varepsilon_i z$ with a constant potential V_{0i} and a y-dependent electric field ε_i, as shown in equation (3). Equation (1) is completely separable and has the solution

$$\Psi_\alpha = \begin{cases} (1/\pi H)^{1/2} \mathrm{e}^{\mathrm{i}k_x x} \sin k_{z,\alpha} z [a_{0,\alpha,+} \exp(\mathrm{i}k_{0,\alpha} y) + a_{0,\alpha,-} \exp(-\mathrm{i}k_{0,\alpha} y)] & \text{for } y < 0; \\ (1/2\pi)^{1/2} b_{i,\alpha} \mathrm{e}^{\mathrm{i}k_x x} \left\{ -\dfrac{Bi(-\zeta_i^{1/3} z_{0,i,\alpha})}{Ai(-\zeta_i^{1/3} z_{0,i,\alpha})} Ai[\zeta_i^{1/3}(z - z_{0,i,\alpha})] + Bi[\zeta_i^{1/3}(z - z_{0,i,\alpha})] \right\} \\ \quad \times [a_{i,\alpha,+} \exp(\mathrm{i}k_{i,\alpha} y) + a_{i,\alpha,-} \exp(-\mathrm{i}k_{i,\alpha} y)] & \text{for } y_{i-1} \leqslant y < y_i; \\ (1/\pi H)^{1/2} \mathrm{e}^{\mathrm{i}k_x x} \sin k_{z,\alpha} z [a_{N,\alpha,+} \exp(\mathrm{i}k_{N,\alpha} y) + a_{N,\alpha,-} \exp(-\mathrm{i}k_{N,\alpha} y)] & \text{for } L \leqslant y. \end{cases} \tag{4}$$

E_x ($k_x = \sqrt{2m^* E_x/\hbar^2}$) is the kinetic energy (momentum) in the x-direction, and $E_{y,i,\alpha} = E - E_x - E_{z,i,\alpha}$ ($k_{i,\alpha} = \sqrt{2m^* E_{y,i,\alpha}/\hbar^2}$) is the kinetic energy (momentum) in the y-direction for the ith layer, where $E_{z,i,\alpha}$ is the αth eigenvalue of the z-directional Schrödinger equation of the layer. Ai and Bi are the Airy functions with $\zeta_i = -2em^*\varepsilon_i/\hbar^2$ and $z_{0,i,\alpha} = 2m^*(E_{z,i,\alpha} - V_{0i})/\zeta_i\hbar^2$. $b_{i,\alpha}$ is the normalization constant for the z-directional wavefunction, and $a_{i,\alpha,\nu}$ is the combinatorial coefficient of the ith layer and the αth state, and ν denotes forward (+) or backward (−) motion of carrier in the y-direction.

In the following discussion, the wavefunction of the ith layer is conveniently represented, in Dirac notation, in terms of the bound states combined with the forward (+) and backward (−) transport states,

$$|i\rangle = \sum_{\alpha,\gamma} a_{i,\alpha,\gamma} |i, \alpha\rangle_\gamma, \tag{5}$$

with $\gamma = +, -$. The coordinate representation of the state $|i, \alpha\rangle_\gamma$ has the form

$$\begin{aligned} \langle \vec{r} | i, \alpha \rangle_\pm = {} & (1/2\pi)^{1/2} b_{i,\alpha} \sin k_x x \\ & \times \left\{ -\frac{Bi(-\zeta_i^{1/3} z_{0,i,\alpha})}{Ai(-\zeta_i^{1/3} z_{0,i,\alpha})} Ai[\zeta_i^{1/3}(z - z_{0,i,\alpha})] + Bi[\zeta_i^{1/3}(z - z_{0,i,\alpha})] \right\} \\ & \times \exp(\pm \mathrm{i}k_{i,\alpha} y). \end{aligned} \tag{6}$$

The requirement of current conservation in the direction of transport between two adjacent layers i and $i+1$ gives the multi-channel transfer matrix equation

$$[J_{i,\alpha,\nu;i,\beta,\gamma}][a_{i,\beta,\gamma}] = [J_{i,\alpha,\nu;i+1,\beta,\gamma}][a_{i+1,\beta,\gamma}], \tag{7}$$

which is usually denoted as $T_{2i-1} X_i = T_{2i} X_{i+1}$. The dimensions of the transfer matrix T (the coefficient matrix X) are $2p \times 2p$ ($2p \times 1$) where p is the number of bound states or channels that are considered in the tunnelling problem. The matrix elements in equation (7) are

$$\begin{aligned} J_{i,\alpha,\nu;j,\beta,\gamma} &\equiv {}_\nu\langle i, \alpha | \hat{J}_i | j, \beta \rangle_\gamma \\ &= (\hbar/2m^*)(\gamma k_{j,\beta} + \nu k_{i,\alpha}) \delta_{k_{x,i}, k_{x,j}} O_{i,\alpha;j,\beta} \exp(-\mathrm{i}\nu k_{i,\alpha} y_i) \exp(\mathrm{i}\gamma k_{j,\beta} y_i), \end{aligned} \tag{8}$$

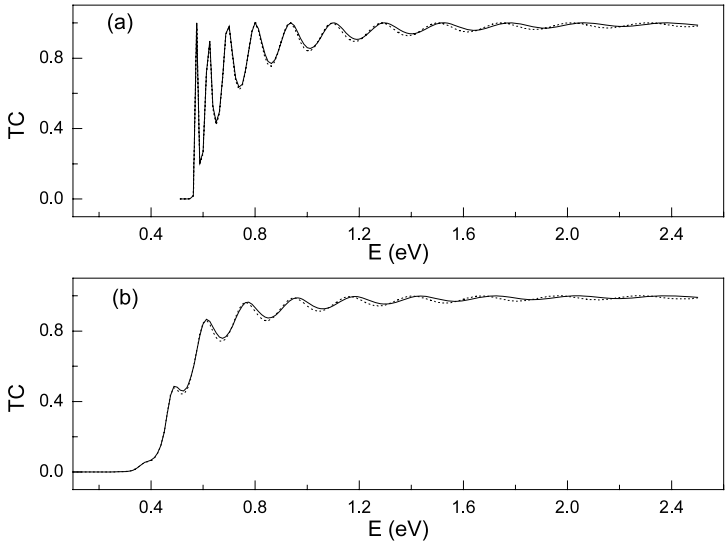

Figure 2. Transmission coefficients calculated by MT (solid lines) and GF (dot lines) methods with the absence of DF for the conditions of (a) $V_{\mathrm{Geff}} = 0$ V and $V_{\mathrm{D}} = 0$ V, and (b) $V_{\mathrm{Geff}} = 0$ V and $V_{\mathrm{D}} = 0.7$ V.

with the overlap integral

$$O_{i,\alpha;j,\beta} \equiv \int_0^h b^*_{i,\alpha} b_{j,\beta} \left\{ -\frac{Bi(-\zeta_i^{1/3} z_{0,i,\alpha})}{Ai(-\zeta_i^{1/3} z_{0,i,\alpha})} Ai[\zeta_i^{1/3}(z - z_{0,i,\alpha})] + Bi[\zeta_i^{1/3}(z - z_{0,i,\alpha})] \right\}^* \times \left\{ -\frac{Bi(-\zeta_j^{1/3} z_{0,j,\beta})}{Ai(-\zeta_j^{1/3} z_{0,j,\beta})} Ai[\zeta_j^{1/3}(z - z_{0,j,\beta})] + Bi[\zeta_j^{1/3}(z - z_{0,j,\beta})] \right\} \mathrm{d}z, \quad (9)$$

where the current operator at the ith interface is defined as $\hat{J}_i = (\hbar/2im^*)[\delta(y - y_i)\vec{\partial}_y - \overleftarrow{\partial}_y \delta(y - y_i)]$, and the arrow $\rightarrow$ ($\leftarrow$) means that the operator operates on the right-hand (left-hand) side. Notably, the overlap $O_{i,\alpha;j,\beta}$ is a measure of the strength of carrier scattering from the bound state α in layer i to the state β in layer j. A non-zero overlap between α and β indicates that a fraction of the longitudinal momentum of the carrier is elastically transferred to or gained from the transverse direction during the carrier transport over these layers. The completeness of the wavefunctions gives the identity $\sum_\alpha O^*_{i,\alpha;j,\beta} O_{i,\alpha;j,\beta'} = \delta_{\beta,\beta'}$, which is useful for gauging the validity of the calculation of the transmission in a system that consists of a finite number of bound states. The transmission coefficient (TC) of the ith channel is defined as the ratio of the total transmission current, that is produced by single-channel injection, to the injection current of the ith channel,

$$\Im_i \equiv \frac{1}{|a_{0,i,+}|^2 J_{0,1,+;0,1,+}} \sum_j |a_{N,j,+}|^2 J_{N,j,+;N,j,+}. \quad (10)$$

The current density at the temperature T can be estimated using

$$J_{\mathrm{D}} = \sum_\alpha \frac{-em^* \sqrt{\pi k_{\mathrm{B}} T}}{\pi^2 \hbar^2} \int_0^\infty \Im_\alpha(E_y) J_{0,\alpha,+;0,\alpha,+}(E_y) \{ Li_{\frac{1}{2}}[\exp(-(E_y - \mu_{\mathrm{S}})/k_{\mathrm{B}}T)] - Li_{\frac{1}{2}}[\exp(-(E_y - \mu_{\mathrm{D}})/k_{\mathrm{B}}T))] \} \frac{1}{\sqrt{E_y}} \mathrm{d}E_y, \quad (11)$$

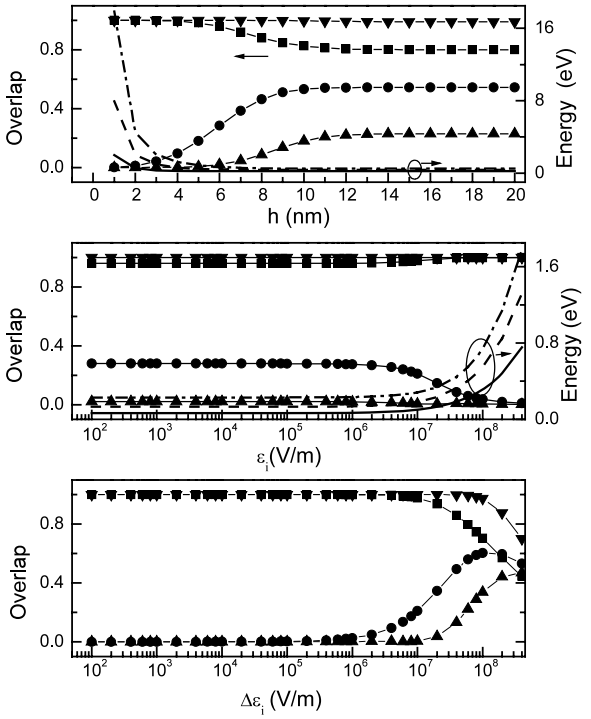

Figure 3. Overlap integrals of the ground state in layer i with ground state $\langle i, 1|i+1, 1\rangle$ (square), the first excited state $\langle i, 1|i+1, 2\rangle$ (circle), and the second excited state $\langle i, 1|i+1, 3\rangle$ (up-triangle) in layer $i+1$ as a function of (a) channel height H for $\varepsilon_i = 1 \times 10^7$ V m^{-1} and $\Delta\varepsilon_i = 5 \times 10^7$ V m^{-1}, (b) electric field ε_i for $H = 10$ nm and $\Delta\varepsilon_i = 1 \times 10^7$ V m^{-1}, and (c) strength of DF $\Delta\varepsilon_i = \varepsilon_i - \varepsilon_{i+1}$ for $H = 10$ nm and $\varepsilon_i = 1 \times 10^7$ V m^{-1}. The energy levels of the ground (solid line), first excited (dashed line), and second excited (dot–dashed line) states as functions of (a) H and (b) ε_i are also plotted. The inverted triangles indicate the completeness of these states.

where Li_n, obtained by integrating the Fermi distribution function over the kinetic energy E_x, is a poly-logarithm function of order n, k_B is the Boltzmann constant, and μ_S (μ_D) is the chemical potential in the source (drain) region.

3. Numerical results and discussion

First, a comparison of the TCs calculated by the MT method (solid lines) with those obtained by the GF method (dashed lines) for the conditions of (a) $V_{\text{Geff}} = 0$ V and $V_D = 0$ V, and (b) $V_{\text{Geff}} = 0$ V and $V_D = 0.7$ V are shown in figure 2. The TCs estimated by the GF approach agree well with those estimated by the MT method.

In a numerical demonstration of the DF scattering, a system with three confined states (a three-channel system) and a gate length $L = 10$ nm is considered. The theory elucidated in the preceding section is applied to the system. The off-diagonal overlaps ($\alpha \neq \beta$) drop as the effective electric field ε_i (figure 3(b)) increases and/or the well width H (figure 3(a)) decreases, saturating at $H > 10$ nm and/or $\varepsilon_i < 3 \times 10^6$ V m^{-1} for $\Delta\varepsilon_i \equiv \varepsilon_i - \varepsilon_{i+1} = 1 \times 10^7$ V m^{-1} (a measure of the DF strength). However, the overlaps increase with the DF strength $\Delta\varepsilon_i$

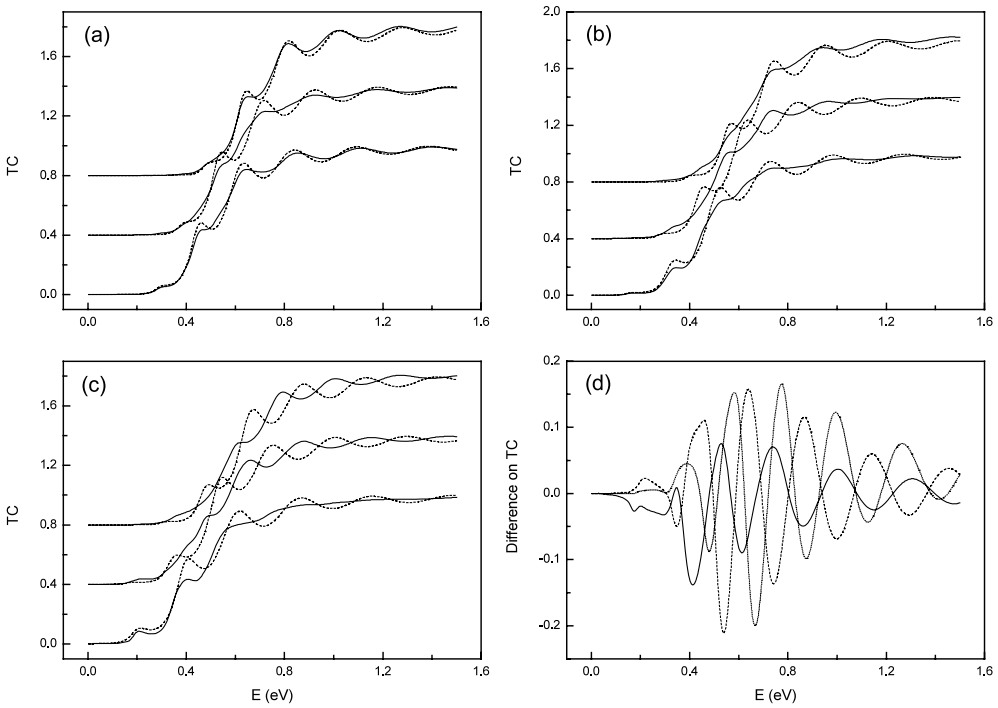

Figure 4. Transmission coefficients of first, second and third (steps of 0.4 from the bottom) channels in the presence (solid) and absence (dashed) of DF scattering for (a) $V_{\mathrm{Geff}} = 1$ V, (b) $V_{\mathrm{Geff}} = 1.5$ V and (c) $V_{\mathrm{Geff}} = 2$ V, and the differences between the TCs in the presence and absence of DF scattering for the first (solid), second (dashed) and third (dotted) channels at biases of $V_{\mathrm{D}} = 0.7$ V and $V_{\mathrm{Geff}} = 2$ V.

(figure 3(c)). These characteristics can be explained by perturbation theory—all of the bound states in each layer form a basis of the transverse Hilbert space, and every state in the nearest-neighbour layers can be expressed as a linear combination of the vectors in the basis. The absolute square of the combinatorial coefficients is the probability that a carrier transitions from one of the states in layer i to the other states in layer j. To a second-order approximation, the transmission is proportional to $|\langle i, \alpha, z|V_{i,j}|j, \beta, z\rangle/(E_{j,\beta,z} - E_{i,\alpha,z})|^2$, where $V_{i,j}$, linearly proportional to $\Delta\varepsilon_i$, is the potential difference between layers i and j, and $E_{i,\alpha,z}$ is the energy of the bound state α in the layer i. The increase of the confinement strength and/or increase in the electric field ε_i increase(s) the energy difference in the denominator of the transmission, as plotted in figures 3(a) and (b), thus reducing the overlaps. The increase in $\Delta\varepsilon_i$ increases the overlaps (figure 3(c)). A non-unity completeness of these states at high DF region displays that higher state (higher than the lowest three states) scattering arises. The contribution from these higher states must be properly accounted for to estimate correctly the transmission in this region.

Equation (10) is utilized to estimate TCs for the lowest three levels (channels), and the calculated results are plotted in figure 4. The TCs in the presence and absence of DF scattering differ substantially and exhibit many features: (1) both cases involve several resonant peaks, because of the quasi-bound states that are produced by boundary reflection at the interfaces between the source and the Si channel and between the drain and the Si channel.

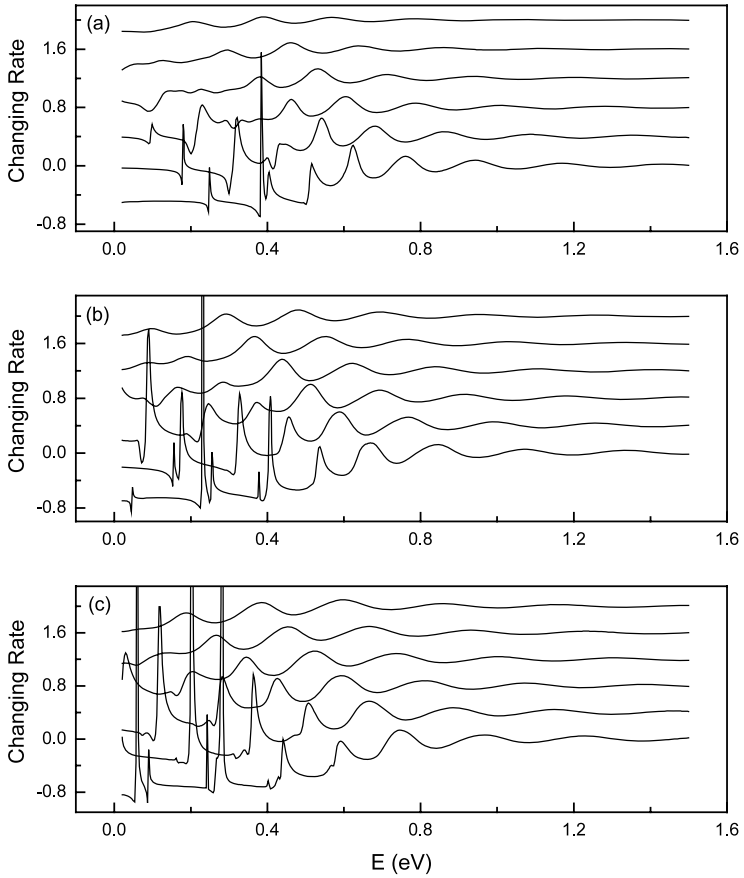

Figure 5. Rate of change of TC for the first channel in the presence and absence of DF scatterings at (a) $V_{\text{Geff}} = 1$ V, (b) $V_{\text{Geff}} = 1.5$ V, and (c) $V_{\text{Geff}} = 2$ V at the biases of $V_{\text{D}} = 0.1$, 0.3, 0.5, 0.7, 0.9, and 1.1 V, in steps of 0.4 from the bottom.

(2) The TC of the ith channel falls as the total energy E of the carrier decreases below its confinement energy $E_{0,i,z}$ in the source region, because no carrier can occupy the tunnelling channel in this situation. The order of the confinement energies for the lowest three levels, $E_{0,1,z} < E_{0,2,z} < E_{0,3,z}$, gives rise to the order of onset energies $E_{\text{os1}} < E_{\text{os2}} < E_{\text{os3}}$ of the TCs. (3) The resonant peaks are broadened by DF scattering, in which some of the transported carriers that are scattered out of the original channel reduce the TC but increase the TC of the other channels, as presented in figure 4(d). (4) Figures 4(a)–(c) indicate the increase in scattering strength with V_{Geff} at $V_{\text{D}} = 0.7$ V because the DF strengths follow the order $\Delta\varepsilon(V_{\text{Geff}} = 2V) > \Delta\varepsilon(V_{\text{Geff}} = 1.5\text{ V}) > \Delta\varepsilon(V_{\text{Geff}} = 1\text{ V})$.

Figure 5 plots the calculated changing rate, defined as $(\text{TC}_{\text{scatt}} - \text{TC}_{\text{nonscatt}})/\text{TC}_{\text{nonscatt}}$, of the first channel, to demonstrate the difference between the TCs in the presence and absence of DF scattering. According to the potential given by equation (3), the DF strength is linearly proportional to $V_{\text{Geff}} - V_{\text{D}}/2$, and the rate of change increases with V_{Geff} but falls as V_{D} and/or the total energy E increase(s). Since carriers with energies of around the Fermi energy E_{fs} in the source region dominate the tunnelling current, a large decrease in the rate of change, caused by DF scattering, markedly degrades the tunnelling current as shown in figure 6.

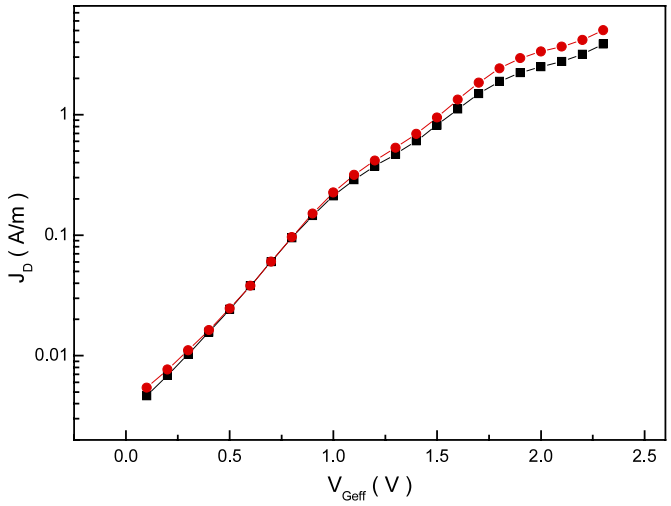

Figure 6. Calculated current density of the drain with the presence (square) and the absence (circle) of DF as a function of V_{Geff} at $V_{\mathrm{D}} = 1.3$ V.

4. Conclusion

A multi-channel transfer matrix theory was derived for carrier transport in the ns-MOS, based on the finite-element approach. Although the derived theory utilizes a simple and screening-free potential (see footnote 5), the consequences calculated herein indicate that DF scattering is important, especially in the ballistic transport region, and that the drop in TC exceeds 50% at low energy. An accurate estimate of the transport current in nanodevices should not ignore the effect of DF scattering, especially in a strong field.

Acknowledgments

The authors would like to express their appreciation of Dr S Datta for providing the computer program for the current calculation using the GF approach. This work was supported by the National Science Council of the Republic of China, Taiwan, under Contract No. NSC95-2623-7-151-003-D.

References

[1] Khanna V K 2004 *Phys. Rep.* **398** 67 and references therein
[2] Chau R, Kavalieros J, Roberds B, Schenker R, Lionberger D, Barlage D, Doyle B, Arghavani R, Murthy A and Dewey G 2000 *IEDM Tech. Digest. International* p 45 http://www.intel.com/
[3] Naveh Y and Likharev K K 2000 *IEEE Electron Device Lett.* **21** 242
[4] Facer G R, Kane B E, Dzurak A S, Heron R J, Lumpkin N E, Clark R G, Pfeiffer L N and West K W 1999 *Phys. Rev.* B **59** 4622
[5] Kohler S, Lehmann J and Hanggi P 2005 *Phys. Rep.* **406** 379 and references therein
[6] Sze S M 1985 *Physics of Semiconductor Devices* 2nd edn (New York: Wiley)
[7] Koga J, Ishihara T and Takagi S-I 2003 *IEEE Electron Device Lett.* **24** 354
[8] Hung K-M and Wu G Y 1992 *Phys. Rev.* B **45** 3461
[9] Wu G Y, Hung K-M and Chen C-J 1992 *Phys. Rev.* B **46** 1521
[10] Dignam M M 1994 *Phys. Rev.* B **50** 2241

[11] Ren Z, Venugopal R, Datta S and Lundstrom M 2000 *IEDM Tech. Digest. International* p 715
[12] Datta S 2000 *Superlatt. Microstruct.* **28** 253
[13] Djeffal F, Chahdi M, Benhaya A and Haliane M L 2007 *Solid-State Electron.* **51** 48
[14] Datta S 1995 *Electronic Transport in Mesoscopic Systems* (Cambridge: Cambridge University Press)
[15] Schwinger J 1991 *Quantum Kinematics and Dynamics* (Redwood City, CA: Addison-Wesley)
[16] Mahan G D 1981 *Many-Particle Physics* (New York: Plenum)